Hindawi Publishing Corporation
Advances in Materials Science and Engineering
Volume 2015, Article ID 387153, 8 pages
http://dx.doi.org/10.1155/2015/387153

Research Article

An Impact Vibration Experimental Research on the Pretension Rectangular Membrane Structure

Jianjun Guo,[1,2,3] Zhoulian Zheng,[2,3,4] and Song Wu[1]

[1] *Chongqing Water Resources and Electric Engineering College, Chongqing 402160, China*
[2] *School of Civil Engineering, Chongqing University, Chongqing 400045, China*
[3] *Key Laboratory of New Technology for Construction of Cities in Mountain Area (Chongqing University), Ministry of Education, Chongqing 400045, China*
[4] *Chongqing Jianzhu College, Chongqing 400072, China*

Correspondence should be addressed to Zhoulian Zheng; zhengzl@cqu.edu.cn

Received 27 November 2014; Accepted 7 January 2015

Academic Editor: Ana S. Guimarães

The pretension of the membrane is applied with biaxial tension bracket; the digital dynamometer is used for measuring the change of the tension; the concentrated impact load is applied on the surface of rectangular membrane; the displacement change of each feature point on the membrane surface is measured by noncontact laser displacement sensor. Through this experiment, the vibration displacement-time curve of the rectangular membrane under the fixed boundary condition is obtained. Further, the vibration frequency is given, according to the power spectral density function. The results of the experimental research are used to verify and correct theoretical formula and make the foundation for further theoretical research.

1. Introduction

The tensioned membrane structure is a new form of Architectural Structures, which is made of soft fabric and clenched by flexible cables or rigid supports to produce stiffness and cover a large space. Membrane structure plays an important role in the public buildings; it not only provides a spacious and comfortable interior space for humans, but also maximizes blending with the natural environment; it not only meets the human's pursuit of the art for architecture, but also achieves good economic benefit.

At present, experts and scholars have made a lot of research work about the mechanical properties of the membrane structure at home and abroad. Xu et al.'s [1] study shows the pretension of membrane structures has a great influence on the load effect and the effect is not linear relationship with load. Chen et al. [2] used the nonlinear stochastic simulation time-history analysis method to analyze the wind-induced vibration response characteristics of ridge-valley membrane structure. Their study concluded that (1) the pretension of the membrane surface not only has a great influence on the shape of the ridge valley membrane structure, but also has a significant influence on the dynamic performance of the structure; (2) with the increase of the pretension, the stiffness of the structure is increased and the mean and standard deviation of displacement response are significantly reduced; (3) with the increase of the pretension, the mean and standard deviation of stress increment caused by wind load are correspondingly reduced, but the total stress (including pretension) is increased; only its rate of increase is small; therefore, increasing the initial pretension of the membrane structure can significantly improve the dynamic performance of the structure. On the basis of form finding and structural characteristics theoretical analysis of cable-reinforced membrane structures, which is subjected to different pretension, the reference standard of the pretension values for cable-reinforced membrane structures is suggested by Cai [3]. Lu [4] used the secondary development technology of ANSYS to make loaded analysis of membrane structures. And his study concluded initial pretension, rise-span ratio, and boundary constraint have an important influence on the deformation of membrane structures under load. In practical engineering, the pretension of membrane structures is generally assumed to be between 5% and 10% of the design strength of the membrane structure and the safety factor is taken to be 5 [5]. Xu et al. [6] used Finite Element Analysis and the actual loading test to make the mechanical property test of the membrane structure under centrally distributed loads, and the result is that the maximum displacement of the numerical simulation is smaller than the maximum displacement of the experiment, while the maximum stress and strain of the former is larger than those of the latter. Added-mass estimation is a key issue in wind-induced vibration of membrane structures [7].

The Jaumann strains and stresses were used to derive a total-Lagrangian finite-element model of membranes by Young et al. [8]. Results from finite-element analyses of an inflated circular cylindrical Kapton tube and a tensioned rectangular Kapton membrane were verified by experiments using a scanning laser vibrometer and a motion analysis system. The nonlinear vibration analysis of a prestretched hyperelastic annular membrane under finite deformations was completed by Soares and Gonalves [9]. The mathematical modeling for the nonlinear vibration analysis of a pretension hyperelastic annular membrane under finite deformations is presented. A parametric analysis of the nonlinear frequency-amplitude relations, resonance curves, bifurcation diagrams, and basins of attraction shows the influence of the initial stretching ratio and membrane geometry on the type and degree of nonlinearity of the hyperelastic membrane under large amplitude vibrations. The same problem is also analyzed using the finite element method. Shin et al. [10] used the extended Hamilton principle and the Galerkin method to compute the natural frequencies and mode shapes for the out-of-plane vibration of the moving membrane. The dynamics of a circular membrane with an eccentric circular areal constraint was studied under arbitrary initial conditions. Alsahlani and Mukherjee [11] presented a method for accurately computing the eigenfrequencies, mode shapes, and modal coefficients needed for dynamics simulation. The vibrational properties of a membrane with linear variation in density along a diameter have been studied by Buchanan [12], the mathematical problem was formulated in polar coordinates, and subsequently numerical results were obtained using a finite element that was formulated in polar coordinates. Frequency of vibration was reported in tabular format and some mode shapes were presented as contour plots of the membrane deflection. Based on the uniaxial and biaxial tension tests data, Dinh et al. [13] proposed a new elastoplastic model for coated fabric which can exhibit the nonlinearities, orthotropic effect, and permanent strains in the constitutive behaviour of this architectural material. Filipich and Rosales [14] solved the natural vibrational problem of nonhomogeneous rectangular membranes by a direct method approach. Two different base functions that belong to complete sets are inserted in the governing functional. Then the variational approach gives the necessary equation to solve the eigenvalue problem. Both the trigonometric and the algebraic sets exhibited an excellent performance, giving between 4 and 5 digits of accuracy with only 10 terms. Kolsti and Kunz [15] presented the development of a numerical model for geometrically nonlinear membranes and evaluated its performance for membranes at static equilibrium. Their scheme has several features not commonly seen in structural Finite Element Analysis: the point collocation method, group formulation, and a staggered mesh. And the resulting system of nonlinear equations is solved with a Jacobian-free Newton–Krylov solver.

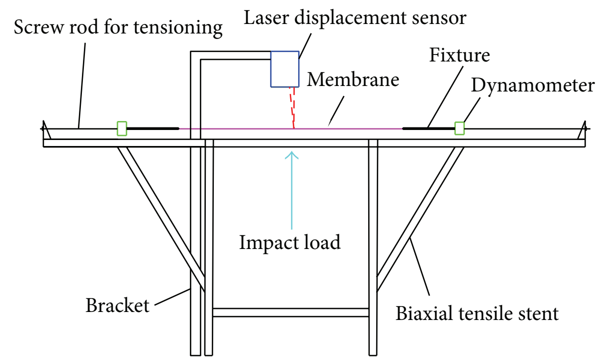

Figure 1: The schematic for experiment.

In summary, many domestic and foreign experts and scholars engaged in research in membrane structures, but they tend to concentrate on theoretical analysis and numerical simulation of membrane structures. The experimental research about membrane structures is very few; specifically the impact vibration research of membrane structures has almost no expert to do. The key problem is how to accurately measure the displacement, stress, and other parameters in the experiment for membrane structures [16].

In this paper, according to the dynamic response characteristics of the membrane structure under the impact loading, with experimental methods, the relationship among pretension size, impact load size, and dynamic response characteristics is suggested. The experimental results can be used to compare with the theoretical calculation and numerical simulation.

2. Devices and Fabric Membranes for Experiment

The experiment was finished on the biaxial tensile stent, in which the plane dimension was 3800 mm × 4160 mm. The schematic of the experiment is shown in Figure 1. The impact load is applied to one side of the membrane; the ZLDS100 laser displacement sensor is arranged to the other side, in order to measure the lateral vibration displacement of membrane when it is hit. Displacement sensor bracket and biaxial tensile stent should be independent in order to avoid the displacement sensor disturbed by the vibration of the biaxial tensile stent [17].

During the loading process of the pretension, the digital dynamometer is used to control the size of the pretension, as shown in Figure 2. Since the membrane material is so light and susceptible to be disturbed, when measuring the vibration displacement, the interference of membrane surface vibration, caused by the mass of measuring equipment,

Figure 2: The digital dynamometer.

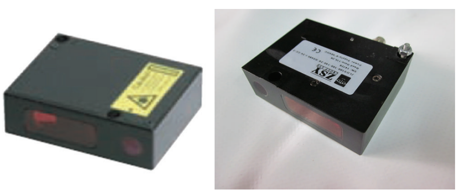

Figure 3: The ZLDS100 laser displacement sensor.

must be considered, and that is why the traditional contact measurement instrument can not be used in this experiment. The ZLDS100 laser displacement sensor is used to measure the vibration displacement of the membrane, as shown in Figure 3. Its performance parameters are precision of 0.1%, sampling frequency of 2 kHz, and resolution of 0.01%.

Three brands of membrane material are used in the tests; they are the Heytex H5573 membrane, the ZZF 3010 membrane, and the Xing Yida membrane, as shown in Figure 4. Mechanical properties of membranes, provided by the manufacturers, are given in Tables 1, 2, and 3.

Membrane material is cut into cruciform specimen; its four ends are cut into stripes, folded, and drilled, respectively, and four corners are rounded, as shown in Figure 5. The central area is a rectangular. At last, loading points (J1, J2, and J3) are marked on the front of the specimen; measurement points (C1, C2, and C3) are marked on the opposite side of the membrane.

Table 1: The material parameters of the Heytex H5573 membrane.

Technical parameters	Technical data
The yarn diameter	1100 dtex high-strength low-polyester filament yarn
Fabric density	12/12 yarn/cm
Thickness	0.80 mm
Gram weight	270 g/m^2
Width	300 cm
Modulus of elasticity (warp/weft)	1720/1490 MPa
Tensile strength (warp/weft)	4400/4200 N/5 cm
Tear strength (warp/weft)	600/550 N/5 cm
Bond strength	>120 N/5 cm
Fire safety standards	German DIN 4102B1, China GB8624 B1
Extreme applicable temperature	(−30)°C~(+70)°C
Light transmittance	8%
Surface treatment	Double-sided PVDF and high self-cleaning coatings

Table 2: The material parameters of the ZZF 3010 membrane.

Technical parameters	Technical data
The yarn diameter	1000 dtex high-strength polyester
Fabric density	12 ∗ 12 cm P2/2
Thickness	0.72 mm
Gram weight	950 g/sq·m
Width	300 cm
Modulus of elasticity (warp/weft)	1590/1360 MPa
Tensile Strength (warp/weft)	4000/3700 N/5 cm
Tear strength (warp/weft)	500/450 N/5 cm
Bond strength	120 N/5 cm
Fireproof performance	B1
Extreme applicable temperature	(−30)°C~(+70)°C
Light transmittance	8%
Surface treatment	PVDF on the front, acrylic on the back

3. Experimental Results

Membrane specimens are made of grade C of polyester fiber membrane material, which is widely used in the actual project. The four sides of the specimen were numbered, x and y are, respectively, labeled on the longitude direction and latitude direction of the specimen. The tension in both directions is equal. The total tension is divided into eight grades, followed by 1 kN, 2 kN, 3 kN, 4 kN, 5 kN, 6 kN, 7 kN, and 8 kN. In each grade of tension, feature points on the surface of the membrane are hit with three kinds of bullets which are launched in two kinds of different guns (Emulational gun with glass bullets, plastic bullets, and iron bullets is marked as FB, FS, and FT, respectively; Toy gun with glass bullets and plastic bullets is marked as WB and WS). The vibration displacement data of three feature points on the membrane surface are acquired with laser displacement sensors. The field test situation is shown in Figure 6.

According to the experimental data, the displacement-time curve of the membrane vibration can be directly plotted. The vibration displacement-time curves of the membrane under the concentrated impact loading are shown in Figure 7. The experimental results show that the vibration process of the membrane is a damping vibration process, and the amplitude is different when the membrane is subjected to different external impact loading.

The Heytex H5573 membrane The ZZF 3010 membrane The Xing Yida membrane

Figure 4: The experimental fabric membranes.

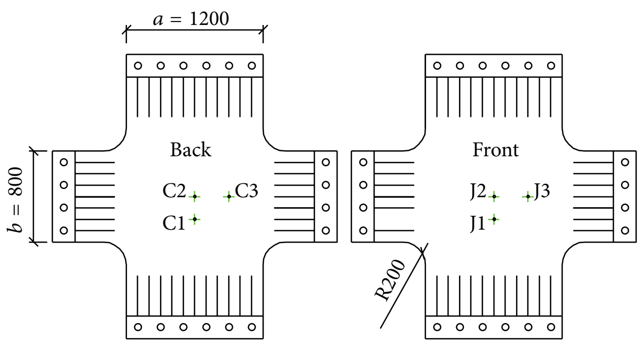

Figure 5: The shape and size of the experimental membrane.

According to the displacement-time curve of the membrane, the displacement power spectral density curve of the membrane could be drawn. The displacement power spectral density curve (Figures 8(a) and 8(b)) corresponds to Figures 7(a) and 7(b). The displacement power spectral density curve of the C1 point for square Heytex membrane with different grades of pretension is shown in Figure 9. Figures 8 and 9 show that the peak vibration frequency of the membrane is significantly improved, when the pretension is increased. The vibration frequencies of the membrane in several kinds of conditions are listed in Table 4 to Table 7.

In order to observe the stress relaxation behavior of architectural membrane suffered tension and impact loads, the changing process of tension was recorded during the test of the rectangle Heytex membrane impacted by the FB. The loss of stretching force is shown in Figure 10.

The $X1$ and $Y1$ are the shown numbers of the digital dynamometer which are read after the pretension is increased immediately. The $X2$ and $Y2$ are the shown numbers of the digital dynamometer which are read when the pretension is increased half an hour later. The $X3$ and $Y3$ are the shown numbers of the digital dynamometer which are read after the surface of architectural membrane is impacted with bullets.

Of course, we also collected vibration displacements of C2 and C3 points. According to the analysis, the changing rules of the vibration displacement-time curves of the C1 point coincide basically with those of C2 and C3 points. The vibration frequency is the same, as shown in Table 6. So we can infer that the vibration form of the membrane is only one, when it is hit by a bullet. However, the maximum vibration amplitude of C1, C2, and C3 points is different, as shown in Figure 11.

Table 3: The material parameters of the Xing Yida membrane.

Technical parameters	Technical data
The yarn diameter	1300 dtex high-strength polyester
Fabric density	36 ∗ 36 cm P2/2
Thickness	0.82 mm
Gram weight	1050 g/sq·m
Width	300 cm
Modulus of elasticity (warp/weft)	1520/1290 MPa
Tensile Strength (warp/weft)	5500/5000 N/5 cm
Tear strength (warp/weft)	600/500 N/5 cm
Bond strength	120 N/5 cm
Fireproof performance	B1
Extreme applicable temperature	(−30)°C~(+70)°C
Light transmittance	7%
Surface treatment	PVDF on the front, acrylic on the back

Table 4: The vibration frequency of the C1 point for square Heytex membrane under the concentrated impact loading (Hz) ($F_{0x} = F_{0y}$, $a = b = 1.2$ m).

Load	F_{0x}							
	1 kN	2 kN	3 kN	4 kN	5 kN	6 kN	7 kN	8 kN
FB	15	19	23	26	28	31	33	35
FS	15	19	23		29			
FT	15	19	23					
WB	15	19	23	26	28			
WS	15	19	23		28			35

4. Experimental Analysis

According to Tables 4 and 5, although the membrane is subjected to different types of impact loadings, the vibration

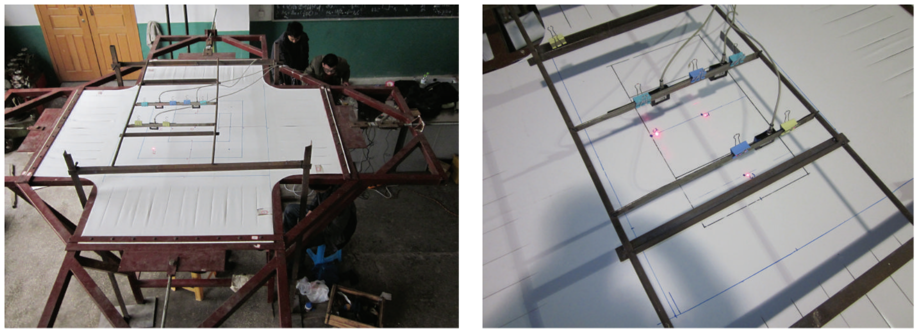

Figure 6: The field test situation.

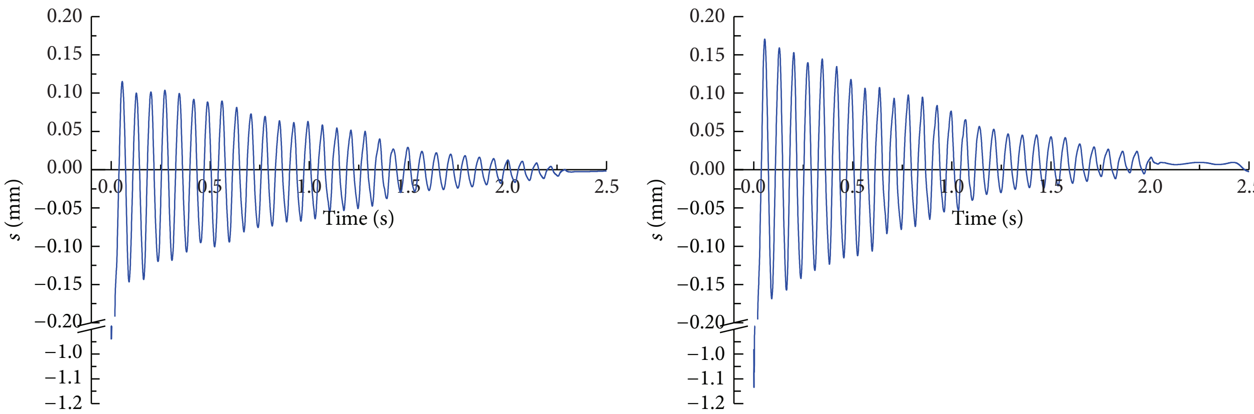

(a) The concentrated impact loading is FB

(b) The concentrated impact loading is FT

Figure 7: The displacement-time curve of the C1 point for square Heytex membrane under the concentrated impact loading ($F_{0x} = F_{0y} = 1$ kN).

Table 5: The vibration frequency of the C1 point for rectangle Xing Yida membrane under the concentrated impact loading (Hz) ($F_{0x} = F_{0y}$, $a = 1.2$ m, $b = 0.8$ m).

Load	F_{0x}							
	1 kN	2 kN	3 kN	4 kN	5 kN	6 kN	7 kN	8 kN
FB	16	20	24	27	30	33	35	37
FS	16	21	24	28	30	33	36	37
FT	15	20	24	27	30	33	35	37
WB	15	20		27	30	33	35	37
WS	15	20	24	27	30	33	35	37

frequency of the membrane is the same, when the membrane is subjected to the same pretension. Table 6 shows that the vibration frequencies of all the three measuring points are the same. This can prove the main vibration mode of the membrane is only one. Figures 8 and 9 also show the power is concentrated in one kind of vibration frequency of the membrane.

So the acquired vibration frequency is the natural frequency of the membrane.

The conclusion can be drawn from Table 7; under the same kind of impact loadings, the vibration frequencies of the two membranes are the same, if their physical parameters are approximate. So the material properties of the membrane are not sensitive to the vibration frequency. It is good news for the measurement of vibration frequencies and the promotion of the membrane structure.

Table 6: The vibration frequency of the points for rectangle Xing Yida membrane under the uniform impact loading (Hz) ($F_{0x} = F_{0y}$, $a = 1.2$ m, $b = 0.8$ m).

Point	F_{0x}							
	1 kN	2 kN	3 kN	4 kN	5 kN	6 kN	7 kN	8 kN
C1	17	21	25	29	31	33	35	
C2	17	21	25	28	30	34		
C3	17	21	25	28	31	33	35	

Table 7: The vibration frequency of the C1 point for square membrane under the uniform impact loading (Hz) ($F_{0x} = F_{0y}$, $a = b = 1.2$ m).

Material	F_{0x}							
	1 kN	2 kN	3 kN	4 kN	5 kN	6 kN	7 kN	8 kN
Xing Yida	14	18	22	25	28	30	32	34
Heytex	15	18	23	25	28	30	33	34

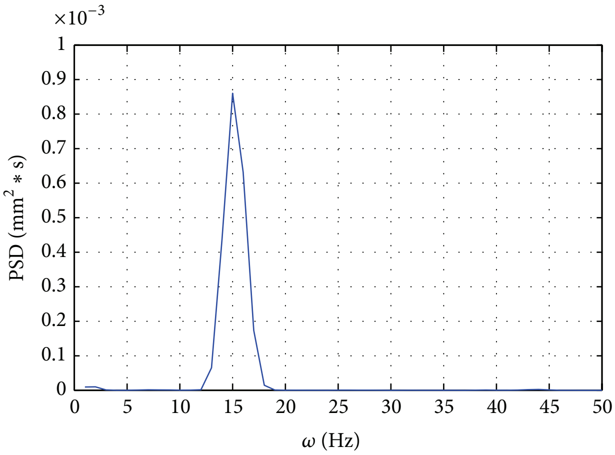

(a) The concentrated impact loading is FB

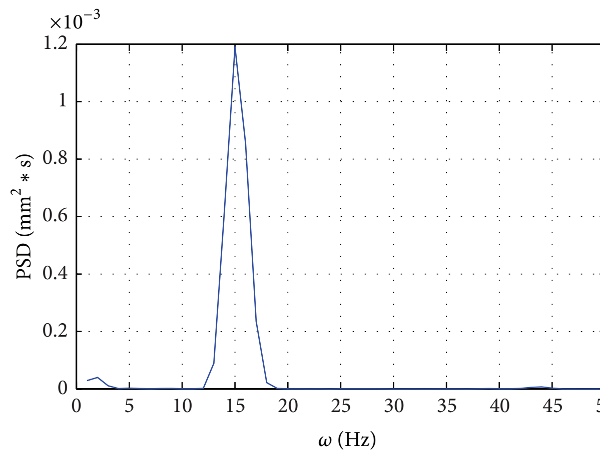

(b) The concentrated impact loading is FT

Figure 8: The displacement power spectral density curve of the C1 point for square Heytex membrane under the concentrated impact loading ($F_{0x} = F_{0y} = 1$ kN).

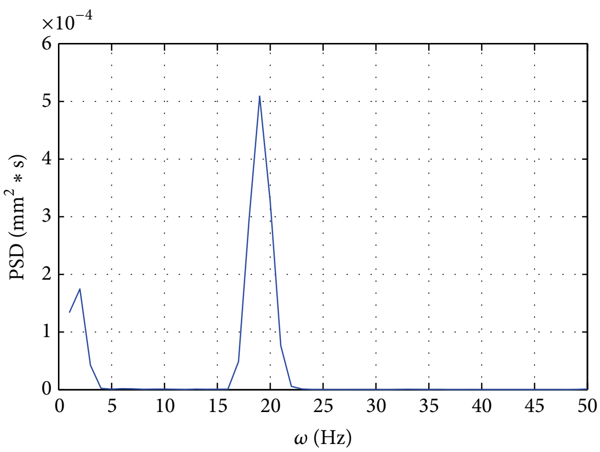

(a) $F_{0x} = F_{0y} = 2$ kN

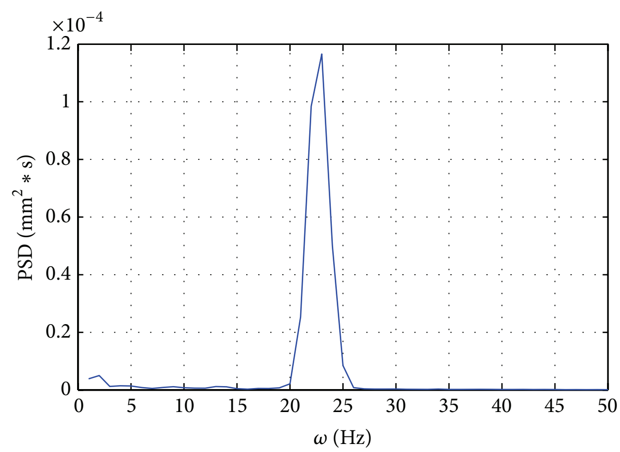

(b) $F_{0x} = F_{0y} = 3$ kN

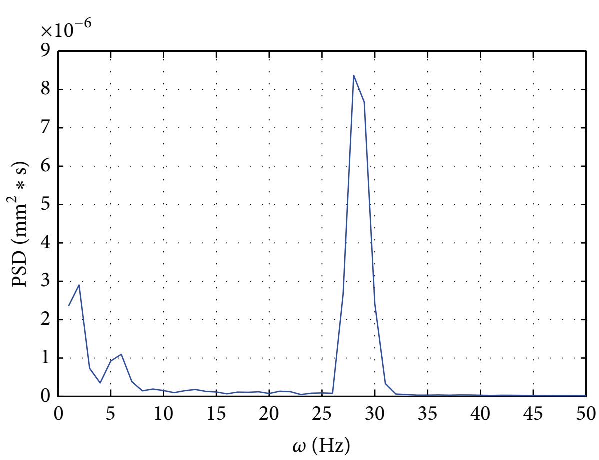

(c) $F_{0x} = F_{0y} = 5$ kN

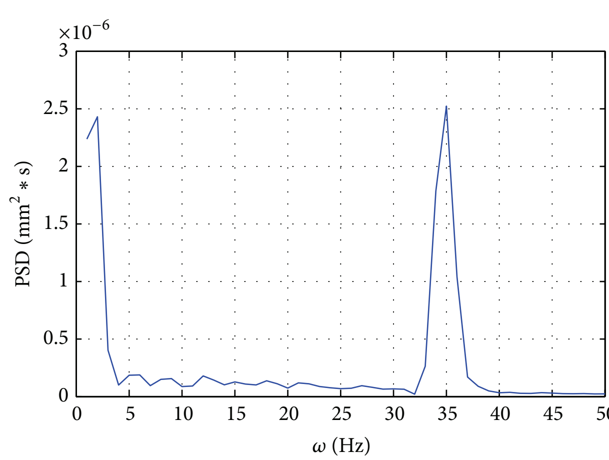

(d) $F_{0x} = F_{0y} = 8$ kN

Figure 9: The displacement power spectral density curve of the C1 point for square Heytex membrane with different grades of pretension.

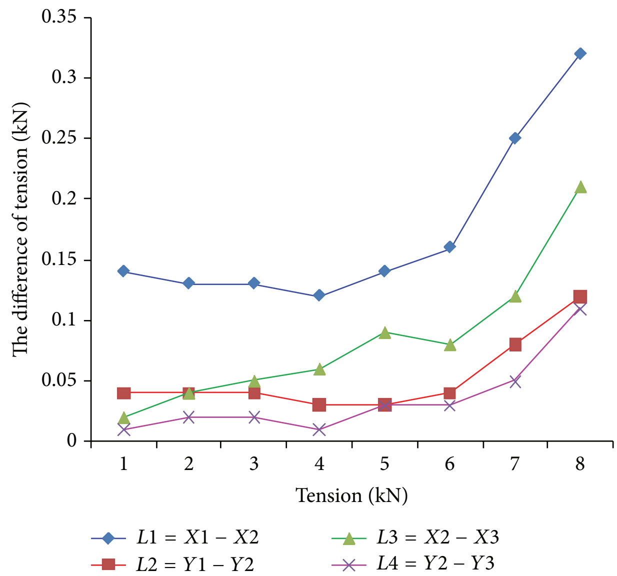

FIGURE 10: The stress relaxation.

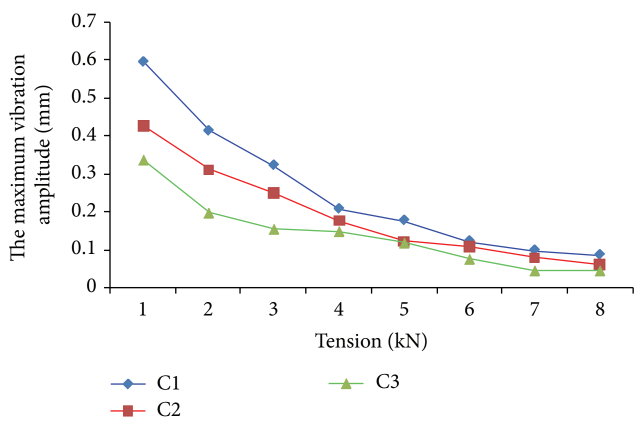

FIGURE 11: The maximum vibration amplitude.

The conclusions can be drawn from Table 4 to Table 7.

(1) When the pretension is increased, the vibration frequency of the membrane increases.

(2) As we all know, $EI = M\omega_0^2$. When the pretension is increased, not only the vibration frequency of the membrane is increased, but also the stiffness of the membrane is increased. However, when the pretension reaches the maximum ($F_{0x} = F_{0y} = 8\,\text{kN}$), the vibration frequency of the membrane is only about 37 Hz.

(3) When the pretension is increased, the increase of the vibration frequency is nonlinear and reduced.

According to Figure 9, the conclusion can be drawn. (1) The loss of tension along weft direction (X) is always much more than that along warp direction (Y). (2) The tension is greater; the loss of the tension caused by impact loading is much more.

These conclusions proved that the pretension can make the stiffness of the membrane increase, but the level of increase is limited. The vibration frequencies of the membrane are given in tables above, which can be used as reference materials for design and construction of tensioned membrane structure.

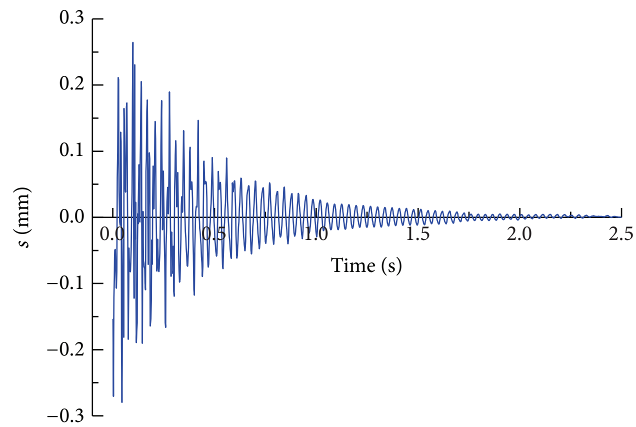

FIGURE 12: The dynamic response time history curves of the building membrane.

In order to provide readers with more references, the displacement-time curves of the membrane are plotted in Figure 12, and the specific experimental conditions are also given. It can be used to compare with the theoretical research of the dynamic response of membranes under impact loading in subsequent research work.

The test conditions for Figure 12 are that the rectangle Xing Yida membrane was hit by the iron bullets which were launched by Emulational gun (FT). Young's moduli are $E_x = 1.52 \times 10^6\,\text{kN/m}^2$ and $E_y = 1.29 \times 10^6\,\text{kN/m}^2$. The aerial density of the membrane materials is $\rho = 1.05\,\text{kg/m}^2$. The rectangle membrane's thickness is $h = 0.82\,\text{mm}$. The side length of the membrane is $a = 1.2\,\text{m}$ and $b = 0.8\,\text{m}$. The quality of the bullet is $M = 8.8 \times 10^{-4}\,\text{kg}$. The speed of the bullet is $v_0 = 16.69\,\text{m/s}$. The pretension of the membrane is $N_{0x} = F_{0x}/a = 5\,\text{kN}/1.2\,\text{m} = 4166.667\,\text{N/m}$ and $N_{0y} = F_{0y}/b = 5\,\text{kN}/0.8\,\text{m} = 6250\,\text{N/m}$.

5. Experimental Conclusions

(i) Since the vibration displacement of the tensioned membrane is very small and the quality of the membrane is very light, the vibration of the tensioned membrane is easy to be disturbed. So we used the contactless laser displacement sensor to measure the vibration displacement of the membrane instead of traditional contact displacement sensors which are always used for measuring the displacement of building structures. This approach can provide a reference for other experimental studies of vibration microdisplacement of similar building structures.

(ii) We analyzed the vibration of tensioned membrane which is subjected to different kinds of pretension and impact loading. The displacement-time curve, displacement power spectral density curve, and vibration frequencies of the membrane were got.

(iii) The pretension can make the stiffness of the membrane increase, but the level of increase is limited.

(iv) The successful experiment proved that this method can be used to measure the parameters of the dynamic characteristics of the membrane and provided foundation for the development of measuring device for tensioned membrane structure.

Conflict of Interests

The authors declare that there is no conflict of interests regarding the publication of this paper.

Acknowledgment

This research presented in this paper was supported by the National Natural Science Foundation of China (Project no. 51178485).

References

[1] Q. G. Xu, J. H. Su, D. J. Han et al., “Discussion for several issues of tensioned membrane structure during load analysis,” *Special Structure*, vol. 21, no. 4, pp. 9–12, 2004.

[2] B. Chen, Y. Wu, and S. Z. Shen, “Wind-induced response analysis of wave-shaped membrane structures,” *Spatial Structure*, vol. 10, no. 3, pp. 41–45, 2004.

[3] W. Q. Cai, *Morphological Analysis Design and the Static Performance Study of Cable-Membrane Structure*, Zhejiang University, Hangzhou, China, 2006.

[4] J. H. Lu, *Study and Improvement of the Dynamic Relaxation Method of Cable-Reinforced Membrane Structures*, Huazhong University of Science and Technology, Wuhan, China, 2006.

[5] X. M. Yin, C. M. Zhu, M. X. Wang et al., “Design of the gymstand’s cable-films structure,” *Industrial Construction*, vol. 36, no. 1, pp. 581–584, 2006.

[6] M. H. Xu, D. K. Liang, and S. J. Zheng, “An experiment research on mechanical capability of cell structure made of PVDF-coated architecture membrane,” *Journal of Experimental Mechanics*, vol. 21, no. 2, pp. 220–224, 2006.

[7] L. Q. Yuanqi, L. Wang, Z. Y. Shen, and Y. Tamura, “Added-mass estimation of flat membranes vibrating in still air,” *Journal of Wind Engineering and Industrial Aerodynamics*, vol. 99, no. 8, pp. 815–824, 2011.

[8] L. G. Young, S. Ramanathan, J. Hu, and P. F. Pai, “Numerical and experimental dynamic characteristics of thin-film membranes,” *International Journal of Solids and Structures*, vol. 42, no. 9-10, pp. 3001–3025, 2005.

[9] R. M. Soares and P. B. Gonalves, “Nonlinear vibrations and instabilities of a stretched hyperelastic annular membrane,” *International Journal of Solids and Structures*, vol. 49, no. 3-4, pp. 514–526, 2012.

[10] C. Shin, J. Chung, and W. Kim, “Dynamic characteristics of the out-of-plane vibration for an axially moving membrane,” *Journal of Sound and Vibration*, vol. 286, no. 4-5, pp. 1019–1031, 2005.

[11] A. Alsahlani and R. Mukherjee, “Dynamics of a circular membrane with an eccentric circular areal constraint: analysis and accurate simulations,” *Simulation Modelling Practice and Theory*, vol. 31, pp. 149–168, 2012.

[12] G. R. Buchanan, “Vibration of circular membranes with linearly varying density along a diameter,” *Journal of Sound and Vibration*, vol. 280, no. 1-2, pp. 407–414, 2005.

[13] T. D. Dinh, A. Rezaei, L. de Laet, M. Mollaert, D. van Hemelrijck, and W. van Paepegem, “A new elasto-plastic material model for coated fabric,” *Engineering Structures*, vol. 71, pp. 222–233, 2014.

[14] C. P. Filipich and M. B. Rosales, “Vibration of non-homogeneous rectangular membranes with arbitrary interfaces,” *Journal of Sound and Vibration*, vol. 305, no. 4-5, pp. 582–595, 2007.

[15] K. F. Kolsti and D. L. Kunz, “A point collocation method for geometrically nonlinear membranes,” *International Journal of Solids and Structures*, vol. 50, no. 2, pp. 288–296, 2013.

[16] C. H. M. Jenkins and U. A. Korde, “Membrane vibration experiments: an historical review and recent results,” *Journal of Sound and Vibration*, vol. 295, no. 3–5, pp. 602–613, 2006.

[17] Z. Zhou-Lian, L. Chang-Jiang, G. Wen-Chuan et al., “A new method—ejection method for nondestructive online monitoring of the pretension of building membrane structure,” *Structural Control and Health Monitoring*, vol. 20, no. 4, pp. 445–464, 2013.